



HAL
open science

NMR and MRI observation of water absorption/uptake in hemp shives used for hemp concrete

Marine Fourmentin, Pamela Françoise Faure, Philippe Pelupessy, Vincent Sarou-Kanian, Ulrike Peter, Didier Lesueur, Stéphane Rodts, Daniel Daviller, Philippe Coussot

► **To cite this version:**

Marine Fourmentin, Pamela Françoise Faure, Philippe Pelupessy, Vincent Sarou-Kanian, Ulrike Peter, et al.. NMR and MRI observation of water absorption/uptake in hemp shives used for hemp concrete. Construction and Building Materials, 2016, 124, pp.405-413. 10.1016/j.conbuildmat.2016.07.100 . hal-01784862

HAL Id: hal-01784862

<https://enpc.hal.science/hal-01784862>

Submitted on 23 May 2018

HAL is a multi-disciplinary open access archive for the deposit and dissemination of scientific research documents, whether they are published or not. The documents may come from teaching and research institutions in France or abroad, or from public or private research centers.

L'archive ouverte pluridisciplinaire **HAL**, est destinée au dépôt et à la diffusion de documents scientifiques de niveau recherche, publiés ou non, émanant des établissements d'enseignement et de recherche français ou étrangers, des laboratoires publics ou privés.

NMR and MRI observation of water absorption/uptake in hemp shives used for hemp concrete

M. Fourmentin^{1,5}, P. Faure¹, P. Pelupessy², V. Sarou-Kanian³, U. Peter⁴, D. Lesueur⁵, S. Rodts¹, D. Daviller⁶, P. Coussot¹

1. Université Paris-Est, Laboratoire Navier (ENPC-IFSTTAR-CNRS), Champs-sur-Marne, France

2. Ecole Normale Supérieure, Département de Chimie, Paris, France

3. Conditions Extrêmes : Matériaux à Haute Température et Irradiation, Orléans, France

4. LHOIST Recherche et Développement, Nivelles, Belgium

5. LHOIST France, Paris, France

6. BCB Lhoist Sud Europe, Besançon, France

Abstract: Hemp concrete used as a construction material is known to provide excellent thermal insulation and hydric regulation, and prevents condensation. Initial water content in the hemp and water exchanges between hemp and binder play a major role in these processes. Here we study how hemp absorbs liquid water. In that aim we rely on ¹H NMR (Nuclear Magnetic Resonance) measurements which make it possible to distinguish water situated inside from water situated outside the hemp. Then, following the evolution of the distribution of NMR relaxation times we are able to quantify the effective amount of water entering the hemp as a function of time. We show that such a measure is better controlled than usual techniques such as weighing an immersed sample or the TC (Technical Committee) RILEM (Réunion Internationale des Laboratoires et Experts des Matériaux, systèmes de construction et ouvrages) method which cannot easily distinguish water inside hemp from water situated outside or wetting the external hemp surface. The water absorption in hemp occurs in two steps: about half the water enters the material in a time of the order of a minute, while the second half of water slowly penetrates over a time of the order of three days. Finally, from ¹H micro NMR imaging we show that the first step corresponds to water entering the pith while the second one corresponds to water diffusing in the wood part of the shiv.

1. Introduction

Current environmental problems lead us to develop more environmentally friendly materials. In particular new concretes are used that contain vegetal aggregate. Hemp shives are a by-product resulting from the pulping of hemp stalks. They were originally used as animal bedding, and since the early 1990, they are also used as aggregates in hemp concrete in which the binder is often a mix of cement and hydrated lime. From a 'life-cycle assessment' perspective hemp construction materials are far more interesting: hemp is naturally produced, does not require much energy to process, does not require maintenance and consumes CO₂ to grow, making the hemp concrete a carbon-negative construction material [1]. Moreover hemp concrete has very interesting properties: it is very light, provides excellent acoustic absorption, thermal insulation and hydric regulation, and prevents condensation. The remarkable physical properties of this material are attributed to its specific multi-scale porous

46 structure [2]: a micro-porosity in the hemp shiv and in the mineral matrix (paste), a meso-
47 porosity due to the presence of air in the paste and a macro-porosity due to voids in the
48 binder-hemp packing. However, the exact mechanisms at work behind these properties are not
49 yet well understood. In particular the thermal and mechanical properties of hemp concrete
50 depend on moisture content so that it is critical to follow and understand the moisture
51 transport in hemp concrete [3-4].

52
53 Although moisture transfers inside hemp concrete are known to have a significant role on
54 their properties they are poorly understood, in particular because it is hard to have
55 straightforward information on the water distribution inside the sample. The hygroscopic
56 behavior of hemp was the subject of several works [5-8]. In fact it is well known that hemp
57 can rapidly absorb large amounts of water during material preparation (up to 3 times its own
58 weight) but the basic mechanisms of liquid water absorption are not well understood. Then, as
59 cement needs water to hydrate, there can be a competition for water between the binder and
60 hemp shives. This water absorption is at the origin of a lack of workability of the concrete a
61 few minutes after the mix. It might also be at the origin of an incomplete hydration of the
62 binder that is sometimes observed and leads to very poor mechanical properties. However it
63 was also suggested that the incomplete hydration is due to a physico-chemical incompatibility
64 between the binder and the plant aggregate [9]. Another explanation In that case the
65 compression strength of the hemp concrete can drop by a factor ten as compared to the usual
66 value when this effect does not occur. Therefore, we need to understand how water transfers
67 between the different phases of the sample. Such information will also have some interest in
68 other fields where hemp is used although these applications often focus on hemp fibers [10-
69 13]. At last it was suggested that liquid water absorption has a greater influence than the
70 vapour diffusion resistance on the moisture and heat transfers in wall components [14].

71
72 Previous works in that field are relatively scarce. Usual measurements consist to immerse
73 some hemp in water and take it out and weigh it after different times of immersion [15]. The
74 standard RILEM measurement is based on such an approach, with in addition a centrifugation
75 preceding each weighing. Note that the centrifugation allows removing a part, but not all, of
76 the free water wetting hemp shives (i.e. the water lying along the external surface of the hemp
77 shives), and the remaining amount is unknown, so that there subsists a significant uncertainty
78 on the effective water mass inside the hemp sample which itself forms a porous medium (see
79 below). One study attempted to measure the capillary rise in hemp fibers [16], but it is not

80 clear yet whether capillarity effects play the major role in water absorption. However it was
81 also shown that the water absorption in hemp can be influenced by surface treatments [17].

82

83 The existing knowledge on water absorption in wood may be helpful for understanding
84 absorption in hemp. The knowledge in that field is more advanced [18] but still complex:
85 there is a large variability in the processes depending on material type, and it appears that
86 wood cannot simply be considered as a homogeneous porous medium in which water would
87 penetrate as a straight front due to capillary effects. Like hemp shives, wood is composed of
88 elongated cells called lumens (i.e. capillaries) which are connected by piths, and water may be
89 found as constitutive, bound or free water. The constitutive water is part of the polymers that
90 constitute the cell walls. Its removal requires high temperatures, which may also lead to the
91 destruction of the material. The bound water is adsorbed inside the cell wall, it is linked by
92 hydrogen bonds to the polymers that constitute the cell wall. Free water corresponds to liquid
93 water inside the lumens. During imbibition of a wood sample, water penetrates in the lumens
94 due to capillary forces and then diffuses in the wall cells under the effect of hydrogen bonds.
95 The penetration of water molecules in the cell walls induces some swelling of the structure.

96

97 The question of absorption of water in hemp is complicated by the fact that hemp generally
98 takes the form of a heap of small (centimetric) pieces stacked on each other. As a
99 consequence this is a porous medium with two very different porosities, namely that of the
100 packing and that of each shiv. In the present work, in order to clarify the physical processes
101 occurring during water absorption we study the phenomena at different scales, i.e. that of the
102 packing and that of the shiv. Moreover a simple weighing hardly makes it possible to
103 distinguish the mass of water effectively inside the shives from that just wetting the pieces (i.e.
104 along the external surface of the pieces). ¹H NMR relaxometry of water molecules, which is
105 sensitive to the pore size will appear as a useful tool for distinguishing these different phases.

106

107 Materials and methods are first described (Section 2), then the result of the monitoring of
108 hemp imbibition obtained by weighing an immersed sample are presented (Section 3.1). The
109 results of NMR relaxometry (Section 3.2) are then compared with data obtained from
110 weighing (Section 3.3), and finally the water penetration through μ MRI (Magnetic Resonance
111 Imaging) is directly observed (Section 3.4).

112

113

114 2. Material and methods

115

116 2.1 Materials

117

118 We mainly use a hemp "Chanvribat" provided by BCB (Balthazard & Cotte Bâtiment)
119 Tradical, which was retted before grinding. Typical particle size is around 1 cm length and 2
120 mm width. Hemps from various origins were also used to compare our measurement methods
121 with the standard one. They were obtained from three other suppliers: Planet Chanvre,
122 Concrete LCDA, Agrofibre. Hemp shiv is obtained by removing seeds and fibers from the
123 hemp, and the corresponding material is then cut in an industrial device. All four shives used
124 in the present study were directly received from industrial plants and were used as such with
125 no additional treatment. Unless explicitly pointed out, here the hemp is used without
126 preliminary drying. We preferred to follow this approach because drying is known to affect
127 the water absorption properties of wood materials, and the former properties are recovered
128 only after a long time. Here, since our material has been left a long time at ambient humidity
129 (about 50% on average) and due to the large hygroscopic time scale of such materials we
130 consider that before each test it has reached an equilibrium initial water content of about 10%
131 (this was checked through drying). Such materials will be referred to as dry samples.
132 However we also looked at the impact of a preliminary drying, as will be described below.

133

134

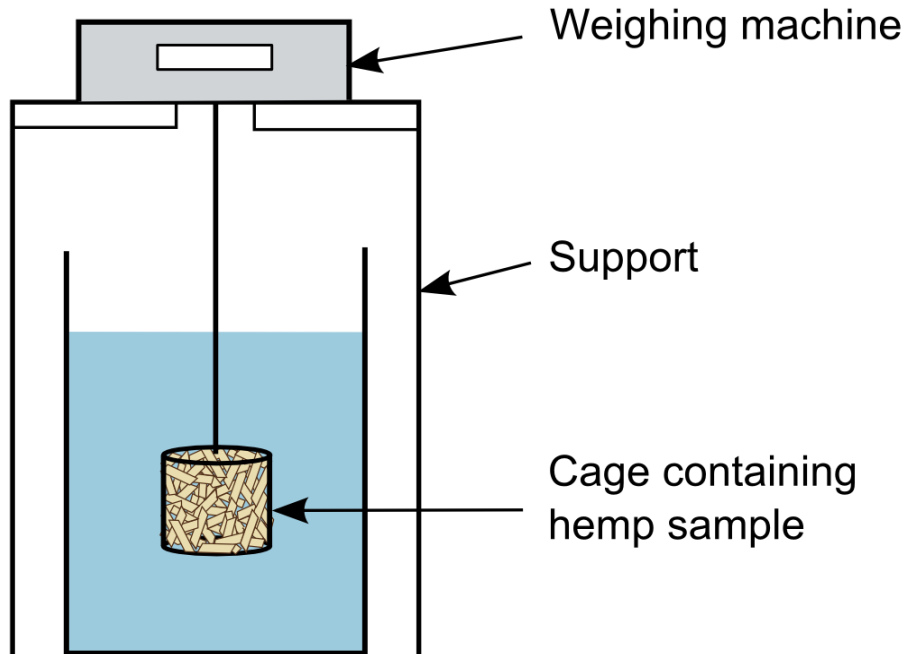
135 2.2 Water absorption followed by direct weighing

136

137 This test aims at measuring the amount of water entering hemp by observing the change of
138 apparent density of a sample immersed in water. For this measurement, hemp is suspended to
139 a scale and immersed in water (see Figure 1). Hemp shives are compacted in a cage of 8 cm in
140 diameter equipped with a screw (allowing the compaction). The center of the sample volume
141 is situated around a depth of 6 cm. The resulting sample mass is 40 g for an apparent volume
142 of 200 to 350 cm³ depending on the imposed pressure. The compaction is such that all hemp
143 shives are in contact with each other, and no shiv behaves loosely, but there still exist small
144 air paths everywhere in the sample so that air escaping from hemp can easily move outside
145 the cage. The cage is made of crossed steel bars leaving holes of about 5 mm. The sample is
146 then suspended via a rigid bar to a scale and immersed in water. And we follow the apparent
147 mass of the sample in time.

148

149



150

151 **Figure 1.** Scheme of the experimental setup used to monitor the water uptake of hemp
152 shives contained in a cage.

153

154

155 The compacted hemp forms a porous system with large pore sizes between the hemp shives.
156 Direct observation of the voids between hemp pieces at the free surface of the sample suggest
157 that the typical pore size inside the medium is of the order of 1 mm, a result consistent with
158 the typical pore size for a packing of compact objects, i.e. a few times smaller than the object
159 size. Let us assume that the dry sample is instantaneously set up at a mean depth of $z = 6$ cm
160 in water. To estimate the water penetration velocity (V) in the sample we can apply Darcy's
161 law:

162
$$V = (K/\mu)\nabla(\sigma \cos\theta/R + \rho gz) \quad (1)$$

163 In which σ is the surface tension of water (here taken as 0.07 Pa.m), θ the contact angle and
164 μ the water viscosity ($\approx 10^{-3}$ Pa.s). Assuming a perfect wetting ($\theta = 0$) and taking a
165 permeability $K = R^2/12$ (as for parallel cylinders of radius $R = 0.5$ mm and of length 4 cm)
166 and considering that the liquid has penetrated over a distance of 4 cm, i.e. the sample radius,
167 we find a velocity of the order of 40 cm.s⁻¹. That means that the water will rapidly penetrate

168 the large pores of the sample (between the shives), i.e. in a time of the order of that needed to
169 fully immerse it. In the following we will assume that this penetration is finished when the
170 other phenomena start to take place.

171

172 Now we can look at the typical velocity of penetration in the vessels of the hemp shiv, whose
173 diameters are typically of the order of 50 μm . Using again (1) with a length of penetration of
174 the order of 1 cm we find a velocity of the order of 2 cm.s^{-1} , which means that the penetration
175 through such channels should also be very fast as compared to our time of observation.

176

177 Let us now assume that the sample has been immersed and the large pores between the hems
178 pieces have been filled with water (mass m_{ext}). Under these conditions the apparent weight
179 (as measured by the scale) of the cage volume is equal to the effective weight
180 $P_{eff} = m_S g + m_W g + m_{ext} g$ minus the buoyancy force $B = \rho V_S g + m_{ext} g$, in which m_S is the
181 mass of solid (i.e. the mass of dry hemp), m_W the mass of water which has entered the hemp
182 shives (and replaced air volumes) since the beginning of the test (we neglect the mass of air),
183 V_S the total apparent volume of the hemp shives and ρ the water density.

184

185 If the hemp shives keep a constant apparent volume, the evolution of the apparent weight will
186 exactly correspond to that of the mass of water entering the hemp shives (and replacing air),
187 i.e. m_W . If the hemp shives swell as a result of some water entrance we will have a variation
188 of the apparent volume $\Delta V_S = m_a / \rho_a$, in which m_a and ρ_a are the mass and density of this
189 specific water. Moreover the effective weight will now include an additional term $m_a g$, and
190 the apparent mass will finally write: $m_W + m_a(1 - \rho / \rho_a)$.

191

192 2.3 TC RILEM protocol for water absorption

193

194 This test aims at measuring the amount of water absorbed by hemp from the change of
195 apparent mass of a hemp sample. This protocol was performed on various hems of different
196 origins within the context of RILEM tests. Shives are dried at 60°C for this measurement.
197 About 25 g of hemp are placed in a synthetic permeable bag with holes of approximately 1
198 mm^2 section area and immersed 1 min in water. The bag is then removed from the water bath
199 and put in a salad spinner which is then rotated 100 times at approximately 2 rpm. At the end

200 the bag containing shives is weighted and then immersed again for 15 min, 4 h and 48 h,
201 before the same protocol of mangling then weighing is applied. The water absorption capacity
202 of the synthetic bag is independently measured. The measurement is repeated 3 times for each
203 hemp with a standard deviation lower than 15%. Here we only present the average value of
204 the water mass divided by the mass of dry hemp.

205

206 2.4 NMR measurements

207

208 Here we intend to follow water absorption from the evolution of NMR signal associated with
209 different pore size in hemp immersed in water. For these measurements, shives had to be
210 grinded in order to enter the experimental set-up. So we first put the hemp in a rotary blade
211 mixer during a short time which allows to get a new shiv size on the order of three times
212 smaller than the initial value. Then this hemp is compacted in a 1 cm thick layer at the bottom
213 of a 18 mm diameter tube and water is added until the water free surface reaches the top of the
214 hemp packing. The initial masses of water and dry hemp are measured before introduction in
215 the tube. In our tests the initial water to hemp mass ratio in the tube was always larger than 5,
216 which means that hemp is in contact with more water than it can absorb, even after a long
217 time. In the following description we consider the initial time as that associated to the first
218 contact between hemp and water in the tube.

219

220 A Bruker Minispec MQ20 ND-Series, with a 0.5 T magnetic field corresponding to a ^1H
221 (proton) resonance frequency of 20 MHz was used for NMR measurements. The probe (3
222 cm^3) was temperature-controlled (20°C) by circulating water. The same apparatus was used to
223 perform both T_1 and T_2 relaxation time measurements.

224

225 In order to get the T_1 distribution, longitudinal proton magnetization decays as a result of the
226 NMR signal relaxation were measured by means of the Inversion Recovery sequence [19],
227 with 50 values of inversion times logarithmically distributed from 0.1 to 12000 ms. Recovery
228 delay was chosen equal to 12 s to ensure complete relaxation of water between two
229 measurements, which implies a measurement duration of approximately 40 min. The sample
230 is left inside the device and the evolution of T_1 is followed during a few days after the first
231 contact.

232

233 The T_1 distribution can then be resolved by means of ILT (Inverse Laplace Transform). Our
234 procedure is a non-negative least square fit to the data with Tikhonov regularization, is similar
235 to the ‘Contin’ method [20-21], and is described in [22]. We finally get an apparent statistical
236 distribution of T_1 , expressed in terms of signal intensity associated with each possible value of
237 T_1 . Typically such a distribution consists of several peaks situated at different T_1 values. Due
238 to the unstable nature and known imperfections of ILT processing [22], such a distribution
239 does not provide a precise description of an effective distribution of T_1 . Two parameters of
240 this distribution nevertheless constitute relevant physical characteristics of the sample:

241

242 (i) The positions of the peak maxima, that we will here call the T_1 values. Roughly
243 speaking these values are related to the mobility of water molecules, and specific
244 interactions of water with their environment (e.g. adsorption, proton exchange with
245 other species, or magnetic interactions at nanoscale). In the particular case of water
246 embedded in a pore cavity, within the usual hypothesis of biphasic fast exchange [23],
247 T_1 scales as the ratio of the volume of free liquid water to the area of the water-solid
248 interface, with a factor depending on the NMR surface relaxivity. Note that this volume
249 to surface ratio is proportional to radius in the case of uniform spherical pores. Thus the
250 T_1 values can be considered as reflecting characteristic pore sizes in the material.

251

252 (ii) The area beneath the part of the curve associated with a peak, which can be considered
253 as proportional to the amount of water within a characteristic pore range.

254

255 Measurements of the transverse relaxation T_2 decays were performed thanks to the Carr-
256 Purcell-Meiboom-Gill (CPMG) sequence. The classical sequence was adapted in order to
257 have a varying value of echo time τ . Thus, the value of echo time is incremented at each echo
258 by multiplying the old value of τ by a low factor. Measurements are done with a recycle delay
259 of 12 s, with 8 scans, with 800 Pi-pulses and pulse separation varying from $\tau = 2.2$ ms to 5 ms.
260 The acquisition time is about 2.6 min. The relaxation time distributions were extracted using
261 the same ILT processing as for T_1 distributions [22]. As for T_1 measurements, each NMR
262 acquisition gives direct information on the quantity of mobile water inside the sample and the
263 T_2 distribution. However the resulting data appeared to be rather noisy so that it is difficult to
264 distinguish clear trends. As a consequence for most of the analysis we decided to focus on T_1
265 data. From T_2 data, which are obtained in a much shorter time, we could at least deduce that
266 an amount of water of the order of the first value observed from T_1 measurements (i.e after

267 several tenths of minutes of imbibition) is already present inside the hemp after a time as short
268 as 2 min.

269

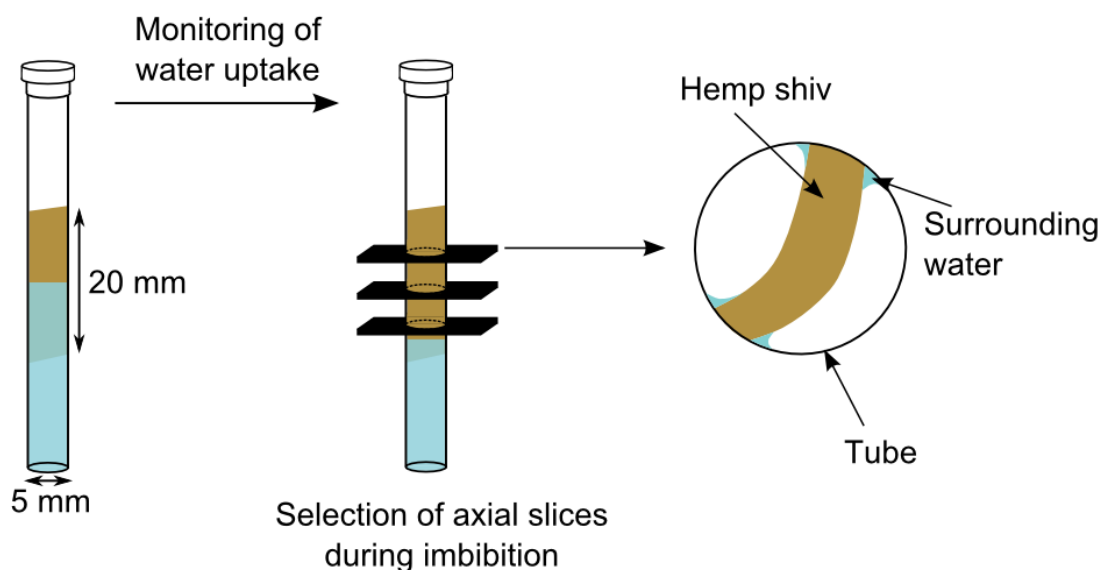
270 2.5 MRI measurements

271

272 Here we intend to have information on water absorption in a hemp shiv from the evolution of
273 the aspect of MR images. The μ -MRI experiments were performed at 17.6 T (^1H Larmor
274 frequency of 750.13 MHz) on a *Bruker Avance IIIHD* spectrometer equipped with a *Bruker*
275 *Micro 2.5* micro-imaging system (100 G/cm for the three axis) and a 10 mm diameter ^1H
276 resonator. Acquisition and data processing were achieved with the *Bruker Paravision 6.0*
277 software. The imaging protocol was carried out using the “Zero Echo Time” sequence (ZTE),
278 [24]) which is particularly dedicated to materials with short transverse relaxation time (T_2^*)
279 such as porous media. 3D images were acquired with a theoretical resolution of 47 μm which
280 took from 9 min to 1 h depending on the number of scans.

281

282 In order to follow the water absorption in one shiv, we used a NMR tube of 5 mm diameter.
283 The shiv is chosen so that its width is around 5 mm. Thus it can be jammed in the tube at a
284 given height with a vertical orientation of the fiber. This jamming is sufficient to avoid any
285 displacement of the shiv even in the presence of strong vibrations possibly induced by the
286 application of the pulsed magnetic field gradients during the measurements. Half the tube is
287 filled with water in such a way that the lower half of the shiv is immersed in water (see Figure
288 2). The MRI sequence allows selecting several cross-sectional slices along the main (fiber)
289 axis of the shiv (see Figure 2). Finally we get (see Figure 2 right) the amount of water in a
290 slice of the sample, with mainly two zones: in hemp and in water surrounding the shiv. Since
291 the water level in the tube decreases in time due to water absorption in hemp, the pure water
292 regions that may be seen in the MRI images soon essentially correspond to residual water
293 menisci left around the shiv. At some time the shiv may lose contact with the outside bottom
294 water but we have no clear information about that.



295

296

297

298

299

300

301

302

303 3. Results and discussion

304

305 3.1 Weighing of an immersed sample

306

307

308

309

310

311

312

313

314

315

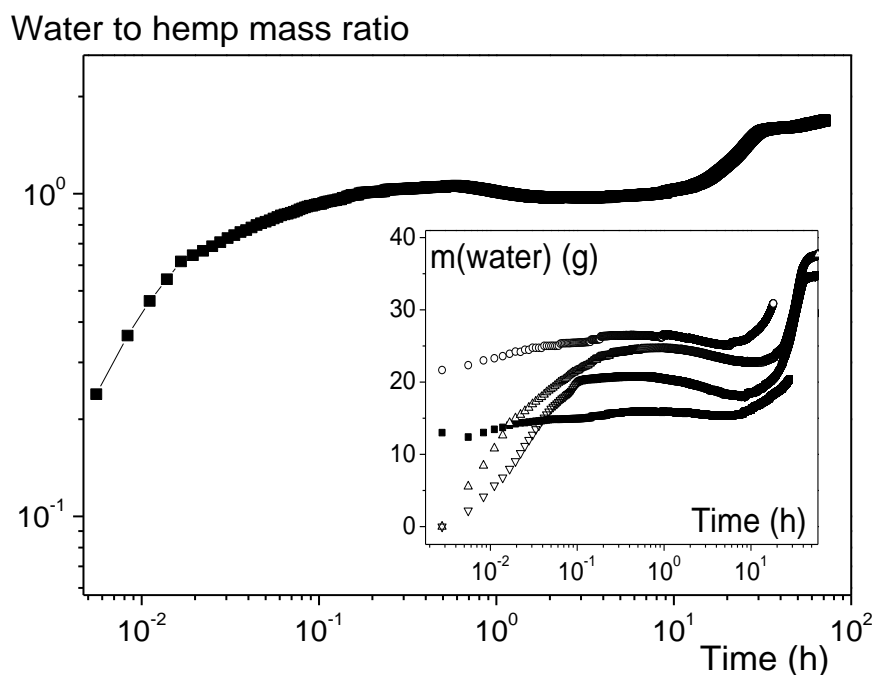
316

317

In Figure 3 we represent the evolution in time of the apparent sample mass divided by the initial mass of dry hemp for such an experiment. The typical curve shape in linear scale over several tenths of hours includes a very fast increase during the first minutes followed by a very slow increase in time over several days. The overall shape of the curve is consistent with the observations reported in literature [25]. Repeating several times such a test with different initial hemp volumes we see that there is a significant variability of the result (inset of figure 3). This is due to the complex effects which occur over a short time: penetration through the porous hemp shiv network and initial imbibition of the hemp. Ideally, i.e. as assumed in the theoretical treatment above, we would need to have the two processes successively so that we could identify the initial time and initial mass at the beginning of imbibition, but since they occur more or less at the same time this is not possible. Under these conditions in the following we will just comment the shape of the imbibition curve.

318
319
320
321
322
323
324
325
326
327

Looking at the detailed evolution in a logarithmic scale we see an intermediate period (say between 1 and 10 hours) where the water mass marks a plateau and even tends to slightly decrease during a few hours before starting again to increase significantly. Such a decrease is surprising because it would a priori means that some water now leaves the hemp pores and is replaced by air, but there is no reason to suddenly invert the process of absorption. Another explanation could be that some air bubbles cannot escape easily from the cage and are jammed between (or stuck to) the particles. However such an effect should lead to a plateau of mass, and not a decrease, since it is equivalent to have no more water entrance in the hemp.



328
329
330
331
332
333

Figure 3. Water to hemp mass ratio as a function of time for hemp sample immersed in water. The inset shows the result of similar tests with different initial hemp volumes in the cage.

334 Another possibility would be a change of water density after absorption in the hemp. Such an
335 effect was suggested for wood: bound water adsorbs to polymers that constitutes cell walls,
336 and only when cell walls are saturated, liquid water fills the cells. Various investigators tried
337 to measure the void volume fraction of wood by immersing wood in different liquids or gases
338 (helium, benzene and water) and measuring the volume of displaced fluid [26]. Benzene was
339 assumed not to enter microvoids in wood, unlike helium. They observed that in the case of

340 wood immersed in helium, the specific volume was lower than for benzene, which confirmed
341 their hypothesis. But in the case of water, the specific volume was even lower than for helium,
342 which means that water does not only enter microvoids. They explain this difference by a
343 compression of water linked to the cell wall by hydrogen bondings. This compression, which
344 corresponds to an increase of water density, might be due both to higher attractive forces in
345 the cell wall than in bulk water and to a reorientation of water molecules. However according
346 to the above equation such a density increase ($\rho_a > \rho$) would induce an increase of the
347 apparent weight of the sample, and not a decrease as observed.

348

349 Finally the only explanation seems to be that there is a kind of transformation of some liquid
350 in gas. Actually such an effect can be observed as soon as water is put in a solid container.
351 After some time one can observe the formation of small bubbles attached to solid surfaces
352 (see for example tap water in a glass). This results from a degassing of solubilized gases (e.g.
353 O_2 , CO_2) at the contact with a solid surface. If the small bubbles thus created remain attached
354 to the shives the hemp sample will appear lighter after some time, as observed in our tests (see
355 Figure 3). Unfortunately we did not find any solution to avoid or control this effect: some air
356 in contact with the liquid may dissolve in it during the test; and removing the ambient gas will
357 tend to accelerate the imbibition.

358

359

360 3.2 Monitoring using NMR

361

362 The weighing of an immersed hemp sample does not allow to get fully reliable data
363 concerning the mass of water entering the pores. Therefore, we use NMR to measure the
364 kinetics of water absorption in hemp.

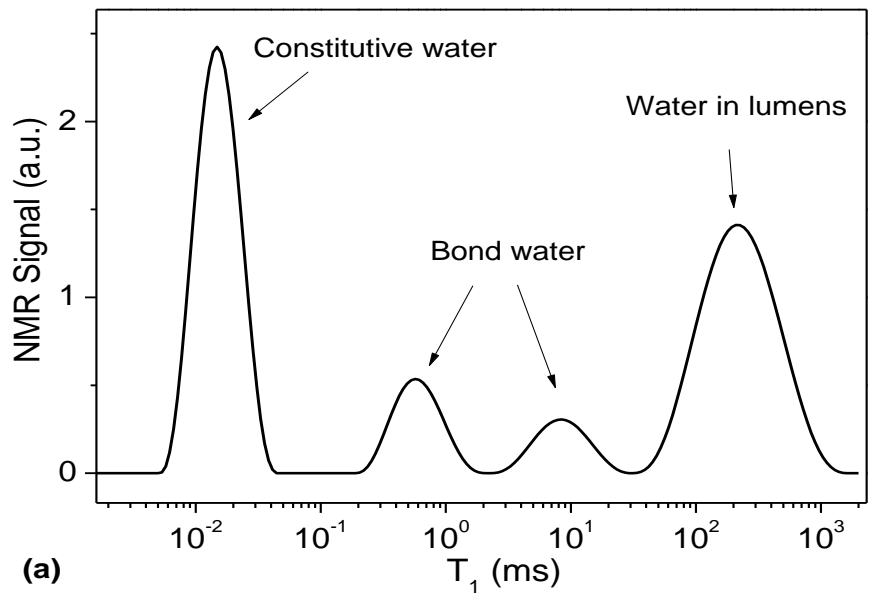
365

366 3.2.1 Various types of water

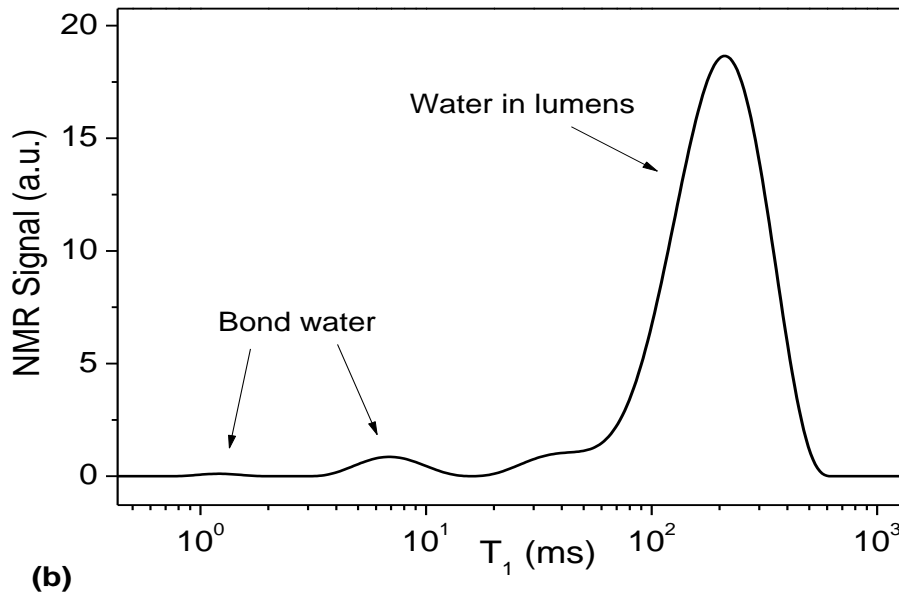
367

368 As we have seen in the introduction three types of water may be considered in wood. Since
369 depending on their environment and the interactions they develop, the spins of the water
370 hydrogen protons exhibit different NMR relaxation times, these different types of water may
371 exhibit different relaxation times. For example, according to Almeida [27], for Douglas fir the
372 transverse relaxation time (T_2) of constitutive water is of the order of a few tens of

373 microseconds, that of bound water ranges from one to a few milliseconds, and that of water in
374 the lumen ranges from ten to a few hundred microseconds.



375
376



377
378

379 **Figure 4:** Distribution of relaxation times for hemp shives under ambient conditions (a)
380 and after immersion in water for 2 min (b)

381
382

383 The distributions of T_1 relaxation time for dry hemp and moisten hemp (2 min immersed
384 sample in water) are presented in Figure 4. Extrapolating the above analysis of water state in

385 wood to this case we can suggest that the peak associated with the smallest relaxation time
386 corresponds to constitutive water, the two central small peaks to bound water and the right
387 peak (i.e. the largest relaxation time) to water in lumens. It is interesting to note that even in
388 this state (hemp under ambient conditions) the signal associated with the three states of water
389 is significant, whereas we could have expected to have negligible water in lumens. However
390 we cannot compare the signal intensity in these three states to that found during absorption
391 because the absolute signal level for two different tests (and different samples), even with the
392 same water amount, generally varies.

393

394 When the hemp shives have been immersed in water for a few minutes (see Figure 4b) the
395 distribution of relaxation strongly differs from that for the “dry” sample. Here we focused on
396 longer relaxation times so that we did not record the signal associated with the constitutive
397 water. The main peak is now the one associated with liquid water in the lumens. We can also
398 remark that the peak associated with the largest relaxation time for bound water has
399 significantly increased with regards to the other peak (lowest relaxation time) for bound water.
400 This illustrates the fact that most water has entered the lumens and a small part of it entered
401 the cell walls but only in the largest pores of these cells.

402

403 3.2.2 Monitoring water absorption (T_1)

404

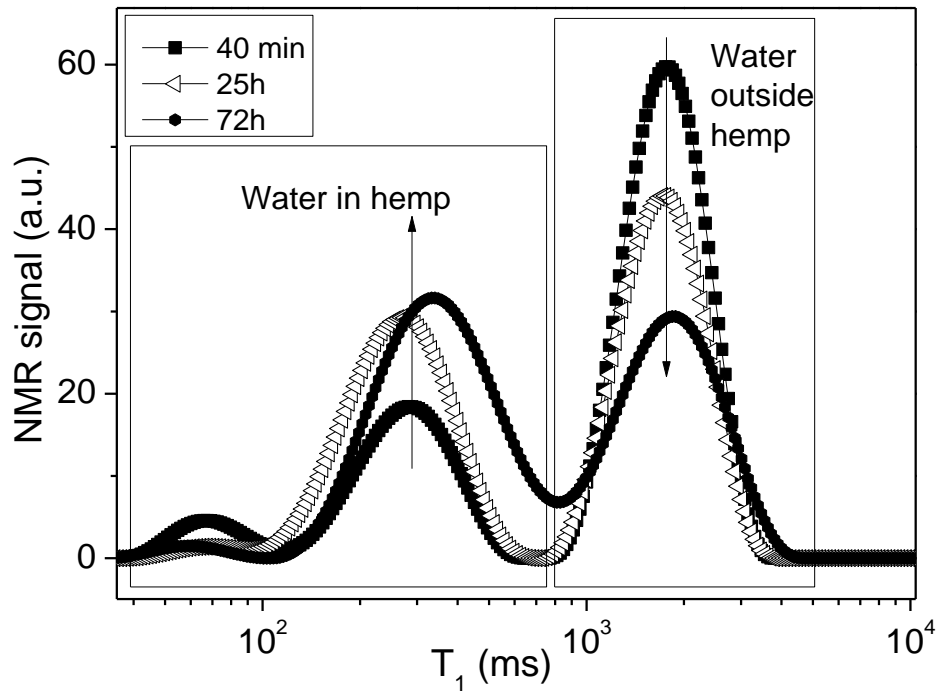
405 We now consider the situation where we have the hemp sample immersed in an excess of
406 (outside) water for a longer time (see procedure in Section 2). The distribution of relaxation
407 times of this system now exhibits two main peaks (see Figure 5), associated with two types of
408 environment. The shortest relaxation time, around 300 ms, is close to the relaxation time of
409 protons in liquid water that we observed previously in moisten hemp. Therefore, it is
410 associated to water in the lumens. The peak corresponding to relaxation times around 2 s
411 corresponds to water outside the hemp. At last we still have a small peak at T_1 below 100 ms
412 which is associated to water bound in hemp, but the signal intensity associated with this water
413 state is much smaller than that in the lumen.

414

415 As the area under each peak is proportional to the amount of water in each type of pore, we
416 can monitor the amount of water that entered in hemp over time. In Figure 5, we can already
417 note that the area beneath the curve part corresponding to water outside hemp seems to
418 decrease while the area associated to water in hemp seems to increase, which corresponds to

419 the transfer of water from outside to inside the hemp shives. Note that the values of the
420 relaxation times associated with each peak slightly change during the process but such
421 changes may be attributed to a side effect of ILT processing, which can shift neighbouring
422 peaks depending on their relative amplitudes [22].

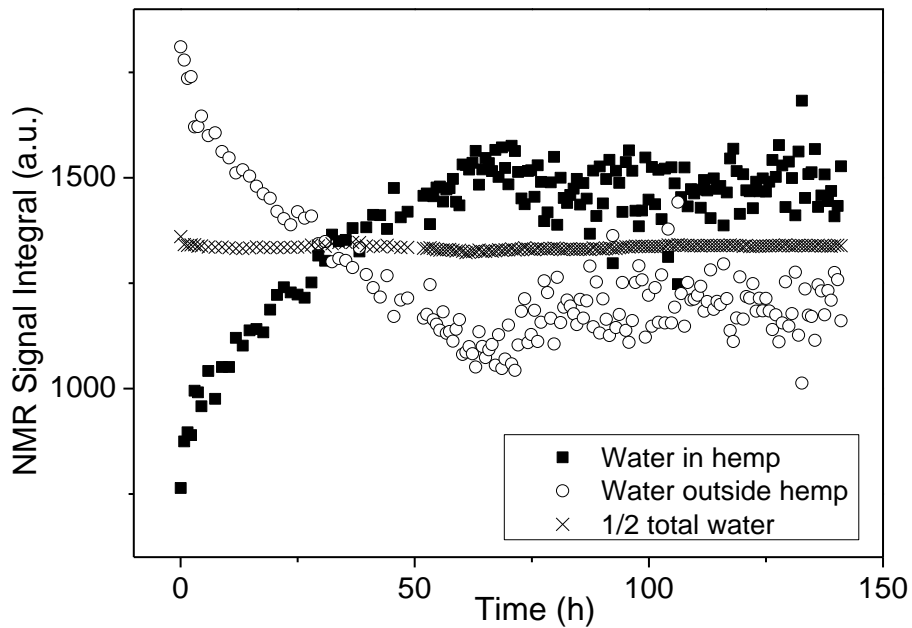
423



424

425 **Figure 5:** Distribution of T₁ relaxation times for a hemp sample put into contact with an excess of
426 water, at three times during the test.

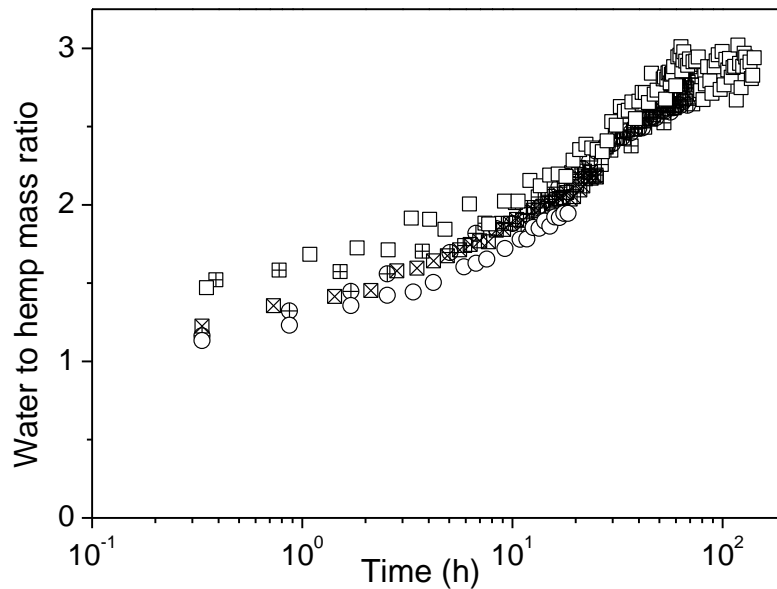
427



428
429
430
431

Figure 6: Evolution of the signal intensities associated to water in hemp and water between hemp particles over time. Half of the total water amount in the sample is also represented.

432 In Figure 6 we show the evolution of the integrated signal for water inside hemp and outside
433 hemp. We see that the signal associated to water in hemp increases in time while the signal
434 associated to water outside hemp decreases. The consistency of this type of measure is
435 demonstrated through the fact that the total water amount deduced from these data remains
436 constant (see Figure 6), as expected since the tube is closed. This in particular confirms that
437 we effectively record the water entering hemp with this technique. We can also notice that the
438 initial signal associated to water in hemp is ten times higher than the signal measured for dry
439 hemp. This confirms that hemp absorbs a significant amount of water during the first
440 measurement.



441
 442 **Figure 7:** Water to hemp mass ratio measured by NMR for different samples (either
 443 crossed or not) either dried (circles) or not (squares). For the dried samples the water to
 444 hemp mass ratio was computed by adding to the hemp mass, and subtracting from the
 445 total water mass, the mass of water lost by drying, so that the data presented here for
 446 dried and non-dried samples can be relevantly compared.

447
 448
 449 The mass of water that is added to hemp is weighted as the sample is prepared. Knowing this
 450 mass allows to calculate the effective amount of water in each phase (inside or outside hemp),
 451 and particularly to determine, for each test, the (linear) relationship between the NMR signal
 452 intensity and the water to hemp mass ratio over time. From such measurements we now have
 453 a view which is in principle not affected by any artefact (in contrast with weighing). The
 454 uncertainty on such data is about 12%, as appears from the repetition of similar tests (see
 455 Figure 7).

456
 457 We also tested the impact of a preliminary drying of the sample which, as already mentioned,
 458 typically withdraws a mass of water equal to about 10% the hemp mass. It appears that this
 459 does not change the general trends of the imbibition (see Figure 7): the data obtained after
 460 drying can be transformed in data equivalent to those without drying by adding to hemp the
 461 additional mass of water associated with drying, and withdrawing this additional mass of
 462 water from the apparent water; the two sets of data appear to be similar to each other within

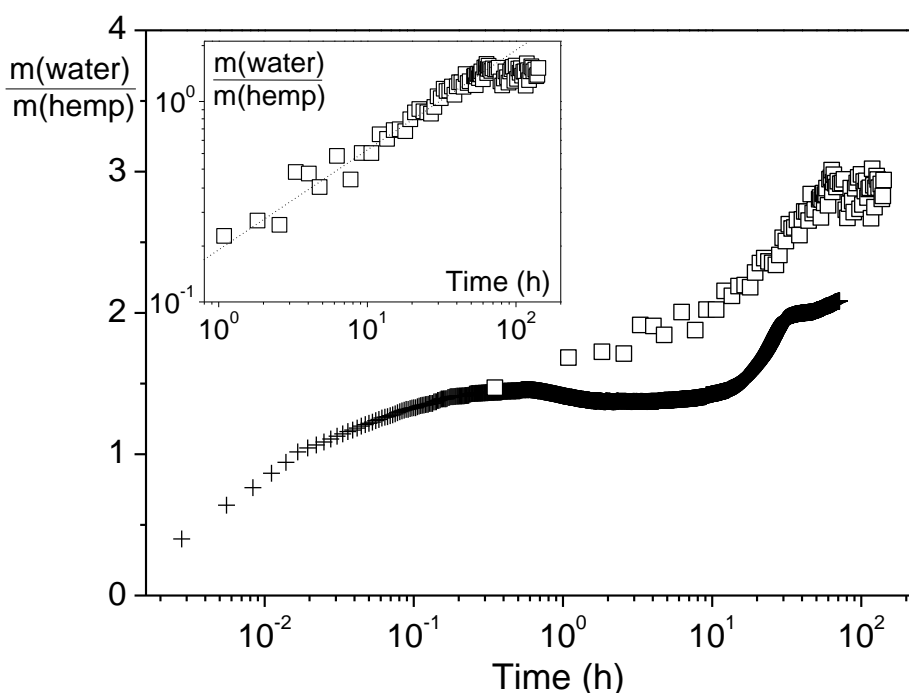
463 the uncertainty on such experiments. Thus it seems that drying has no more effect than simply
464 shifting the initial water mass towards a lower value but this water loss is balanced by a very
465 fast water imbibition at the beginning of the test.

466

467 We see that the hemp has initially (i.e. during the time needed for the first NMR
468 measurement) absorbed a large amount of water of about 150% of the hemp mass. Then it
469 goes on absorbing water during 3 days, until reaching a mass to hemp ratio of about 3 (see
470 Figures 7 and 8). This confirms that hemp imbibition occurs in two phases each of them
471 associated with the absorption of half the total absorbed water: one over short time, i.e. in less
472 than two minutes (as appears from T_2 measurements and weighing), and the other over several
473 days. The first phase likely might correspond to some kind of capillary imbibition in the
474 largest pores, but the entered water does not increase as predicted by a simple Washburn
475 imbibition (i.e. as \sqrt{t}) [28]. In the second phase the mass increase is much slower (i.e.
476 approximately proportional to $t^{1/8}$). However if we consider that in phase 2 the water simply
477 penetrates in a dry region we could expect a Washburn process for the additional water mass
478 (from the penetrated amount at the end of phase 1, i.e. 1.5). And indeed the additional water
479 mass evolves as \sqrt{t} (see inset of figure 8). Actually, anticipating on results of Section 5 this
480 interpretation is in disagreement with MRI observations: during phase 1 the water effectively
481 rapidly invades a first region of each hemp shiv, but during phase 2 it seems to penetrate
482 globally in another region of shiv, instead of progressively invading it from one side. This
483 suggests that in phase 2 there is a slow diffusion process through the hemp structure rather
484 than a capillary penetration.

485

486 We also remark (see Figure 8) that the data from NMR do not show a slight water mass
487 decrease between 1 and 10 h. Instead we now have a slow but regular increase, which
488 suggests that the direct mass measurement of a hemp sample fully immersed in water can be
489 affected by some artefact inducing a significant error on measurements. In the following we
490 will use the NMR data as the reference data for describing the effective water amount
491 absorbed in hemp.



492
 493
 494
 495
 496
 497
 498
 499

Figure 8. Water to hemp mass ratio in time as measured by T_1 relaxometry (squares) and by weighing of an immersed sample (crosses). The inset shows the additional (see text) water to hemp mass ratio in phase 2 of imbibition as a function of time in logarithmic scale. The continuous line has a slope $\frac{1}{2}$.

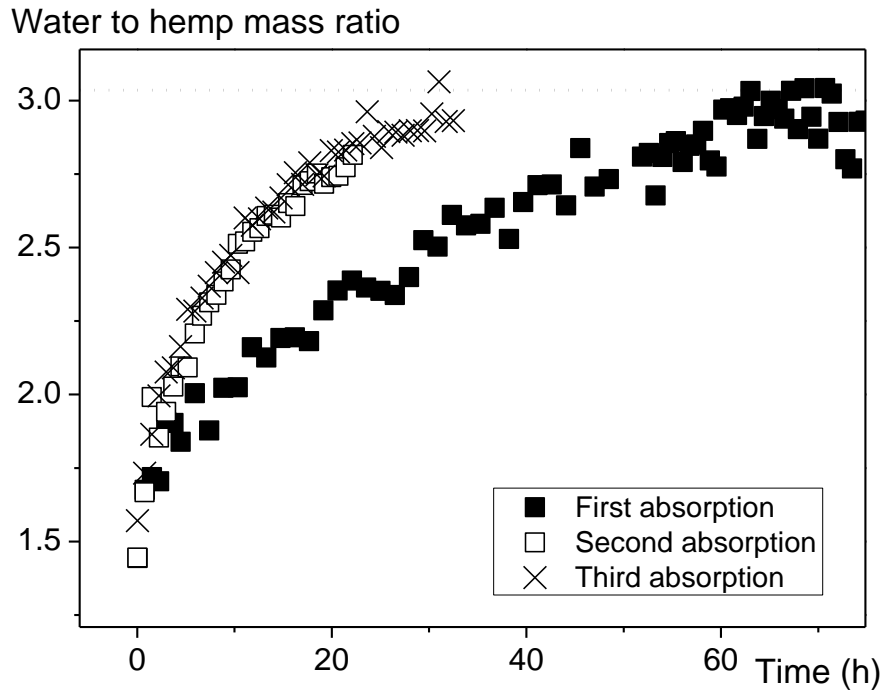
500 3.2.3 Impact of sample history

501

502 Successive imbibition tests were carried out by drying the sample (put in an oven at 60°C
 503 until mass stabilization) after each test. By monitoring by NMR the successive water uptakes
 504 we see that the second imbibition is different from the first one (see Figure 9). The water mass
 505 in hemp increases faster after the first cycle (imbibition + drying), but finally reaches the
 506 same saturation level. In the next cycle the water absorption process is the same as the second
 507 one. This suggests that the structure has been irreversibly modified during the first cycle but is
 508 no more modified in the next cycles. This might be related to the observation that after the
 509 first drying (and not in the subsequent cycles) a brown layer overlays the sample, which likely
 510 corresponds to the extraction of molecules from the hemp possibly playing a role in the initial
 511 imbibition. We also could see that after the first cycle the sample volume has slightly
 512 increased so that it tends to be strongly jammed in the container in which it was initially just

513 packed by hand, which confirms some slight irreversible changes in the structure after the first
514 imbibition.

515



516

517

518 **Figure 9:** Results of the water absorption in hemp shives during successive imbibitions (separated
519 by drying) measured by T_1 -relaxometry.

520

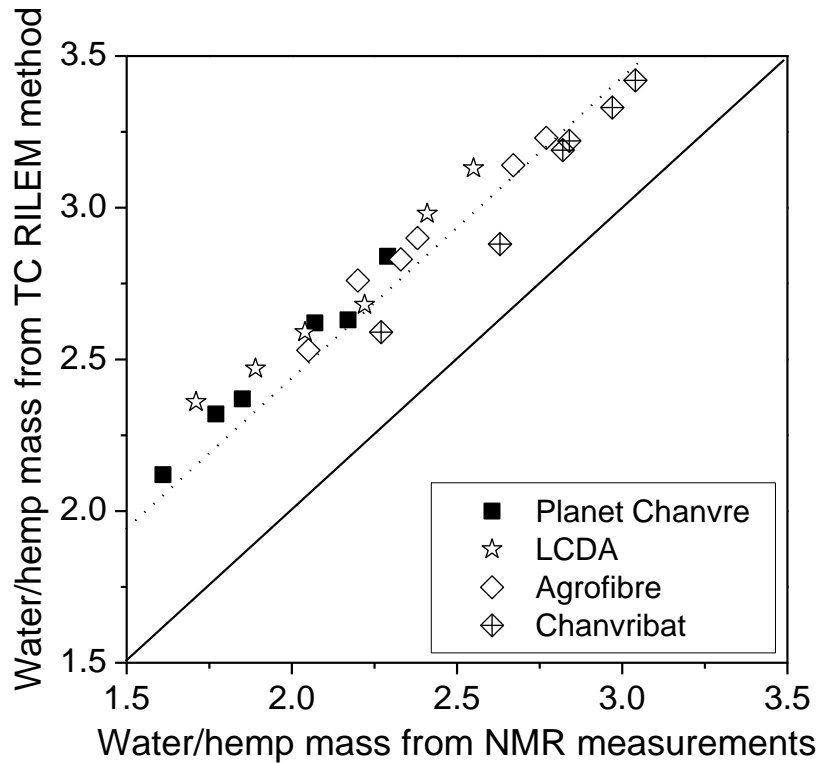
521

522 3.3 Comparison of NMR data with data from TC RILEM method

523

524 We can now compare the results obtained from the TC RILEM method to those obtained by
525 NMR for the four different hems at different times during the imbibition process. Except for
526 one material the mass found by the TC RILEM method is significantly higher than that found
527 by NMR all along the process (see Figure 10). In fact we have a constant shift of the two
528 evolutions, i.e. at any time during the process the water mass found by the TC RILEM method
529 is just simply equal to that effectively entered in the hemp plus a constant term. It is likely that
530 this term exactly corresponds to the water amount remaining at the surface of the hemp shives
531 due to capillary effects. This would give an additional mass of water proportional to the
532 specific (external) surface of the hemp sample, thus proportional (for a given hemp type) to
533 the mass of hemp by a factor α , and consequently an additional term α in the representation

534 of m_w/m_s , in agreement with our data. This factor finally appears (see Figure 13) to vary in a
 535 rather narrow range (0.4-0.6) depending on hemp type.
 536



537 **Figure 10:** Water to hemp mass ratio measured by the TC RILEM method as a function
 538 of that measured by NMR measurements for different hems at different times during
 539 imbibition. The lines have a slope 1, the continuous line would correspond to a perfect
 540 agreement between the two types of measurement.
 541

542

543

544 3.4 Imaging of water absorption

545

546 In order to understand why hemp imbibition takes place in two phases with very different
 547 kinetics, a hemp shiv imbibition is directly observed using μ -MRI. We used the ZTE
 548 sequence [24] which allows detecting protons that have relaxation times as short as a few tens
 549 of microseconds. Therefore, we expect to detect both bound and liquid water. With this
 550 sequence, the signal intensity is proton density weighted, which means that it is proportional
 551 to the local amount of protons. As a consequence, roughly speaking the bright parts of the
 552 images corresponds to the zones with the highest water density.

553

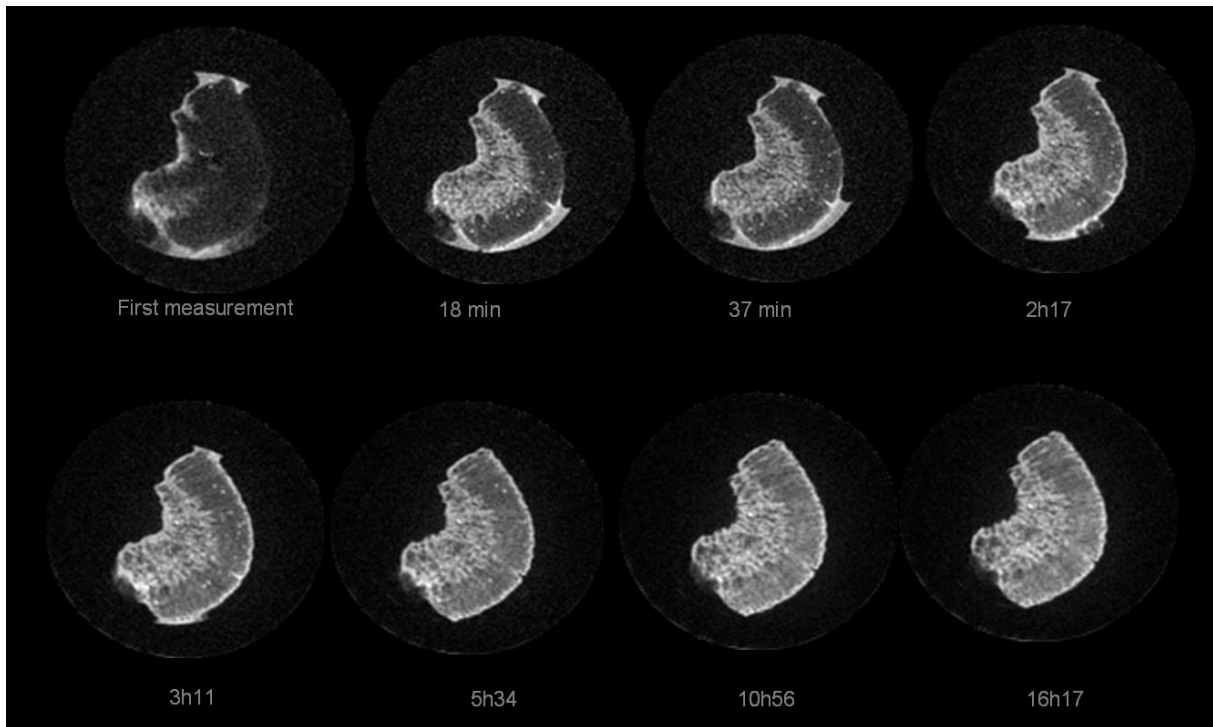
554 We first attempted to get an image of dry hemp but we were unsuccessful, the signal was too
555 low. Images could be obtained when the shiv is in contact with water. In that case the image
556 evolution is qualitatively similar in the different slices along the shiv axis (see Figure 2). Here
557 we focus on one of the central slice to discuss the typical trends. The first image corresponds
558 to signal acquisition during the first four minutes of hemp imbibition. We can see that it is
559 blurred (see Figure 11), which is likely a result of the significant evolution of the water
560 density distribution over the time of acquisition. Indeed in MRI each information at a local
561 scale is not simply the result of the average signal over the total time of acquisition as for
562 several other imaging techniques, here it is based on a reconstruction by Fourier transform of
563 the information obtained from a virtual picture obtained in the field gradient (reciprocal)
564 space. As a consequence significant evolution of the spatial density can lead to this kind of
565 blurring. We can nevertheless still distinguish the contour of the shiv and external water
566 between the shiv and the tube, which are regions in which the water amount changes likely
567 remain negligible.

568

569 In the next step, i.e. the image obtained after 18 min, the picture is better resolved, likely
570 because as we have seen in previous measurements the absorption kinetics during that period
571 is much slower than in the first stage. We can now clearly see the hemp shiv surrounded by
572 water. Moreover the shiv seems to be composed of two parts. The left part is much brighter
573 than the right part. These regions correspond to two different tissues, respectively the pith and
574 the wood. The pith is the youngest part of the stem, it is in its centre. During the plant growth,
575 the pith becomes wood through a lignification process. Lignin forms a three dimensional
576 network that provides its rigidity to the cell wall. It also makes the tissues more hydrophilic.
577 In fact, polysaccharide components of the plant cell wall are highly hydrophilic and thus
578 permeable to water. Lignin makes it possible for the tissue to conduct water efficiently [28].
579 As a consequence, pith is very hydrophilic whereas the woody part is more hydrophobic. This
580 explains that after 18 min, the pith is already very bright whereas the wood does not seem to
581 contain much water. We can also observe some bright points in the woody part of the shiv.
582 They are likely due to some vessels filled with water (which finally represents a small water
583 amount). Indeed the imbibition of wood is known to take place in two successive steps.
584 During a first stage water penetrates through some vessels due to capillary forces. Then it
585 diffuses through vessel walls as a result of hydrogen bonding. Only when these walls are
586 saturated water can stay in the lumens.

587

588 During the next hours, we observe a progressive brightening of the woody part. After 16 h it
589 seems to contain almost as much water as the pith. During that period the water amount in the
590 pith does not seem to evolve significantly. This suggests that the two successive steps in the
591 kinetics of water absorption in hemp as observed from NMR tests results from the successive
592 imbibition of the two different parts of the shiv: first a fast penetration of water in the pith,
593 then a much slower penetration in the wood.
594



595
596
597
598
599

Figure 11: Evolution of the middle slice of hemp during water absorption as seen by MRI.

600 **4. Conclusion**

601

602 We have shown that following the evolution of the distribution of NMR relaxation time
603 makes it possible to quantify the effective amount of water entering the hemp. It is more
604 difficult to use the weighing technique to get relevant data and we were unable to understand
605 the exact origin of some artefacts observed in that case, in particular those leading to a water
606 mass decrease while NMR data show a continuous increase of water mass inside the hemp.

607

608 We also showed that in general the TC RILEM method significantly overestimates the
609 effective water content inside the hemp, an effect likely due to some water remaining along

610 the hemp shiv surfaces as a result of capillary effects. It was also shown that this
611 overestimation is poorly dependent on the hemp type and does not vary in time (i.e. during
612 absorption), so that it can simply be taken into account for a better interpretation of the results
613 of such tests.

614
615 As clearly seen from NMR, water intake occurs in two steps, a fast one taking place in less
616 than two minutes, corresponding to water entering the pith, and a slow one, taking place over
617 days, corresponding to water diffusing into the woody part of the shiv. Further studies could
618 focus on how plant-related parameters (species, growth conditions...) affect the water intake.
619 The effect of additional treatment, like retting could also now be fully assessed. Finally, the
620 way this two-steps kinetics affect the setting of hemp-lime concrete can now be thoroughly
621 studied and taken into consideration in the formulation of hemp concrete relationship /
622 performance.

623

624

625 **Acknowledgement**

626

627 Financial support from the TGIR-RMN-THC Fr3050 CNRS for conducting part of this
628 research is gratefully acknowledged.

629

630

631 **References**

632

633 [1] Boutin MP, Flamin C, Quinton S, Gosse G. Analysis of life cycle of 1. thermoplastic
634 compounds loaded with hemp fibers, and 2. hemp concrete wall on wood structure. French
635 Ministry of Agriculture-INRA Report, MAP 04 B1 05 01 (2005) (in French)

636

637 [2] Collet F, Bart M, Serres L, Miriel J, Porous structure and water vapour sorption of hemp-
638 based materials, *Construction and Building Materials*, 2008;22:1271-1280

639

640 [3] Samri D, Arnaud L, Assessment of heat and mass transfers in building porous materials,
641 Proc. of the 4th European Conference on Energy Performance & Indoor Climate in Buildings,
642 Nov 2006, Lyon.

643

644 [4] Tolkovsky A. *Sorption behaviour of hemp and lime concrete floors*, MSc Architecture:
645 Advanced Environmental and Energy Studies, Graduate School of the Environment,
646 Machynlleth, UK (2010)

647

648 [5] Collet F, Chamoin J, Pretot S, Lanos C, Comparison of the hygric behaviour of three
649 hemp concretes, *Energy and Buildings*, 2013;62: 294-303

650

- 651 [6] Bart M, Moissette S, Oumeziane YA, Lanos C, Transient hygrothermal modelling of
652 coated hemp-concrete walls, *European Journal of Environment and Civil Engineering*,
653 2014;18:927-944
654
- 655 [7] Walker R, Pavia S, Moisture transfer and thermal properties of hemp-lime concretes,
656 *Construction and Building Materials*, 2014;64:270-276
657
- 658 [8] Othmen I, Poullain P, Leklou N, Moisture transfer in three hemp concretes, *Construction*
659 *Materials and Structures* (ed. By Ekolu SO, Dundi M, Gao X, 1st International Conference on
660 *Construction Materials and Structures*, Johannesburg), 2014:1358-1363
661
- 662 [9] Diquelou Y, Gourlay E, Arnaud L, Kurek B, Impact of hemp shiv on cement setting and
663 hardening: Influence of the extracted components from the aggregates and study of the
664 interfaces with the inorganic matrix, *Cement and Concrete Composites*, 2015;55:112-121
665
- 666 [10] Mustata A, Mustata FStC, Moisture Absorption and Desorption in Flax and Hemp Fibres
667 and Yarns, *Fibres and Textiles in Eastern Europe* 2013; 21: 26-30.
668
- 669 [11] Shahzad A, Effects of Water Absorption on Mechanical Properties of Hemp Fiber
670 Composites, *Polymer Composites*, 2012;33:120-128
671
- 672 [12] Rouison D, Couturier M, Sain M, MacMillan B, Balcom BJ, Water Absorption of Hemp
673 Fiber/Unsaturated Polyester Composites, *Polymer Composites*, 2005;26:509-525
674
- 675 [13] Dhakal HN, Zhang ZY, Richardson MOW, Effect of water absorption on the mechanical
676 properties of hemp fibre reinforced unsaturated polyester composites, *Composites Science*
677 *and Technology*, 2007;67:1674-1683
678
- 679 [14] Evrard A, Flory-Celini C, Claeys-Bruno M, De Herde A, Influence of liquid absorption
680 coefficient on hygrothermal behaviour of an existing brick wall with Lime-Hemp plaster,
681 *Building and Environment*, 2014;79:90-100
682
- 683 [15] Stevulova N, Cigasova J, Purcz P, Schwarzova I, Long-Term Water Absorption
684 Behaviour of Hemp Hurds Composites, *Chemical Engineering Transactions*, 2014;39:559-
685 564
686
- 687 [16] Pejic BM, Kostic MM, Skundric PD, Praskalo JZ, The effects of hemicelluloses and
688 lignin removal on water uptake behavior of hemp fibers, *Bioresource Technology*,
689 2008;99:7152–7159
690
- 691 [17] Stevulova N, Cigasova J, Purez P, Schwarzova I, Kacik F, Geffert A, Water absorption
692 behavior of hemp hurds composites, *Materials*, 2015;8:2243-2257
693
- 694 [18] Siau JF, *Transport processes in wood*, Springer-Verlag, Berlin, 2004
695
- 696 [19] Callaghan PT, *Principles of nuclear magnetic resonance microscopy*, Clarendon Press,
697 Oxford, 1991.
698
- 699 [20] Whittall KP, MacKay AL, Quantitative interpretation of NMR relaxation data, *J. Magn.*
700 *Reson.* 1989;84:134–152.

- 701
702 [21] Provencher SW, A constrained regularization method for inverting data represented by
703 linear algebraic or integral equations, *Comput. Phys. Commun.* 1982;27:213–227.
704
- 705 [22] Faure P, Rodts S, Proton NMR relaxation as a probe for setting cement pastes, *Magn.*
706 *Reson. Imaging* 2008;26:1183–1196.
707
- 708 [23] Philippot S, Korb JP, Petit D, Zanni H, Analysis of microporosity and setting of reactive
709 powder concrete by proton nuclear relaxation, *Magn. Reson. Imaging* 1998;16:515–519.
710
- 711 [24] Weiger M, Pruessmann KP, MRI with Zero Echo Time, *Encyclopedia of Magnetic*
712 *Resonance*, 2012, John Wiley and Sons
713
- 714 [25] Arnaud L, Gourlay E, Experimental study of parameters influencing mechanical
715 properties of hemp concretes, *Construction and Building Materials*, 2012;28:50-56.
716
- 717 [26] Stamm AJ, Hansen LA, The bonding force of cellulosic materials for water (from
718 specific volume and thermal data). *Journal of Physical Chemistry*, 1937;41:1007-1016.
719
- 720 [27] Almeida G, Leclerc S, Perre P, NMR imaging of fluid pathways during drainage of
721 softwood in a pressure membrane chamber. *International Journal of Multiphase Flow*,
722 2008 ;34 :312-321.
723
- 724 [28] Washburn EW, The dynamics of capillary flow. *Physical Review*, 1921;17:273-283
725
- 726 [29] Sarkanen KW, Ludwig CH, Lignins: occurrence, formation, structure and reactions.
727 Wiley, New York, 1971.
728